

A long-duration active region: Evolution and quadrature observations of ejective events

H. Cremades^{1,2}, C. H. Mandrini^{3,4}, M. C. López Fuentes³,
L. Merenda¹, I. Cabello^{1,2}, F. M. López⁵ and M. Poisson³

¹Universidad Tecnológica Nacional – Facultad Regional Mendoza, CEDS

²Consejo Nacional de Investigaciones Científicas y Técnicas (CONICET)
Rodríguez 243, 5500, Mendoza, Argentina
email: hebe.cremades@frm.utn.edu.ar

³Instituto de Astronomía y Física del Espacio (IAFE, UBA-CONICET),
Buenos Aires, Argentina

⁴Facultad de Ciencias Exactas y Naturales,
Universidad de Buenos Aires, Buenos Aires, Argentina

⁵Instituto de Ciencias Astronómicas, de la Tierra y del Espacio (ICATE),
CONICET-UNSJ, San Juan, Argentina

Abstract. Unknown aspects of the initiation, evolution, and associated phenomena of coronal mass ejections (CMEs), together with their capability of perturbing the fragile technological equilibrium on which nowadays society depends, turn them a compelling subject of study. While space weather forecasts are thus far not able to predict when and where in the Sun will the next CME take place, various CME triggering mechanisms have been proposed, without reaching consensus on which is the predominant one. To improve our knowledge in these respects, we investigate a long-duration active region throughout its life, from birth until decay along five solar rotations, in connection with its production of ejective events. We benefit from the wealth of solar remote-sensing data with improved temporal, spatial, and spectral resolution provided by the ground-breaking space missions STEREO, SDO, and SOHO. During the investigated time interval, which covers the months July–November 2010, the STEREO spacecraft were nearly 180 degrees apart, allowing for the uninterrupted tracking of the active region and its ensuing CMEs. The ejective aspect is examined from multi-viewpoint coronagraphic images, while the dynamics of the active region photospheric magnetic field are inspected by means of SDO/HMI data for specific subintervals of interest. The ultimate goal of this work in progress is to identify common patterns in the ejective aspect that can be connected with the active region characteristics.

Keywords. Sun: activity, Sun: coronal mass ejections (CMEs), Sun: photosphere, Sun: magnetic fields

1. Introduction

Active regions in the Sun are sites of intense magnetic fields, usually complex and highly dynamic. Within active regions, helical magnetic flux tubes emerge after traversing the convection zone (Schrijver & Zwaan 2000) and are revealed in the photosphere as regions of opposite magnetic polarity, whose complexity may increase as a product of diverse photospheric movements. These displacements drag the footpoints of magnetic field lines building up highly stressed coronal fields (Forbes 2000), while magnetic flux is continuously injected in the corona. Magnetic energy is gradually stored in a quasi-equilibrium state, until it is released by some triggering mechanism, often resulting in

the eruption of a coronal mass ejection (CME). Although active regions are a recognized common source of CMEs, little is known about which circumstances make a particular active region to be the next one to trigger a CME, or when in time this ejection of plasma will take place. Given the potential of CMEs to unleash geomagnetic storms, to find answers to these matters is urgently needed.

Although there are reports on the long-term evolution of the global photospheric magnetic field such as that of by Petrie (2013), on the CME production rate along the solar cycle (e.g. Gopalswamy *et al.* 2013, Riley *et al.* 2006), and on the continuous tracking of an active region while it transits the front side of the Sun (Démoulin *et al.* 2002 & Green *et al.* 2002), there are no precedents on the uninterrupted tracking of a single long-duration active region throughout several solar rotations, much less in connection with its CME production. In this effort, we profit from the simultaneous observations from multiple vantage points provided by the STEREO twin spacecraft (Kaiser *et al.* 2008), together with those from SDO (Pesnell *et al.* 2012), and SOHO (Domingo *et al.* 1995). These observations offer a unique opportunity to examine the CME production of a long-duration active region throughout its life, uninterruptedly and along five solar rotations, in combination with photospheric properties such as magnetic flux and current helicity. In this work, we explore for the first time the eruptive capability of an active region from birth until decay in terms of some of its photospheric characteristics, with the main goal of finding whether active region properties hint at the frequency and properties of the ensuing CMEs.

2. The investigated active region

After the long solar cycle 23, its long and deep solar minimum of over two years, and more than 800 days without sunspots, a series of long-duration active regions emerged on the Sun. The selected active region, which persisted for at least 5 rotations, appeared for the first time on the east limb as active region NOAA 11089 on 19 July 2010. By then, the STEREO twin spacecraft were approaching a quadrature situation with respect to Earth, i.e. reaching the 180 degrees of separation between both spacecraft. At the same time, the SDO mission was just beginning its operational phase, and provided best views of the active region as it crossed the front side of the Sun.

Table 1 resumes the NOAA numbers that were assigned to the active region after a new solar rotation, together with the dates at which the active region appeared on the east limb, was at central meridian, and disappeared on the west limb. This active region has been subject of several independent studies, which address different aspects and different stages of evolution (e.g., Guo *et al.* 2013, Zuccarello *et al.* 2014, Mandrini *et al.* 2014, Cremades *et al.* 2015). In the latter two, the active region NOAA 11121 is analyzed as a complex together with the closely related active region 11123. For that last investigated rotation of the active region lifetime, we considered the ejective aspect of the complex, given their magnetic connectivity and the impossibility to isolate CMEs as originating in one or the other active region.

3. CME productivity

When CMEs propagate along the Sun-observer line, they usually appear in coronagraph images as a total or partial halo that surrounds the coronagraph occulter. Halo CMEs lack structure, are diffuse, and dim (e.g. Lara *et al.* 2006), to such an extent that they may not be detectable. In fact, Cremades *et al.* (2015) found that the coronagraphs at the STEREO spacecraft detected twice as many CMEs propagating towards Earth

Table 1. Overview of the investigated active region. The first column is the AR number, while the second, third, and fourth columns respectively refer to the dates when the AR appeared on the east limb, was at central meridian (CM), and disappeared on the west limb.

AR number	East limb	CM	West limb
11089	2010/07/19	2010/07/25	2010/07/31
11100	2010/08/16	2010/08/22	2010/08/28
11106	2010/09/11	2010/09/17	2010/09/23
11112	2010/10/08	2010/10/14	2010/10/20
11121	2010/11/05	2010/11/11	2010/11/17

than SOHO, for a specific date when these spacecraft were in quadrature. When CMEs propagate towards Earth and are thus potentially geoeffective, their source regions are located close to central meridian and are best observed, but without observations off-set from the Sun–Earth line the accurate identification of the origin site of a solar eruption is still a challenging task. Therefore, to uninterruptedly track the active region under study, as well as its CME productivity, we use simultaneous observations from multiple vantage points.

The location of the active region was decisive to determine which instrument was best to observe the region and its associated eruptive phenomena. When the region was transiting the front side of the Sun, we examined it by means of the 193 Å channel of the Atmospheric Imaging Assembly (AIA; Lemen *et al.* 2012) and of the Helioseismic Magnetic Imager (HMI; Scherrer *et al.* 2012) onboard SDO, while we detected the ensuing CMEs from a quadrature perspective, using the COR2 coronagraph of the STEREO Sun–Earth Connection Coronal and Heliospheric Investigation (SECCHI; Howard *et al.* 2008). Likewise, when the active region was close to the solar limbs, we used the SECCHI Extreme–Ultraviolet Imagers (EUVIs) to track the region activity (EUVI-B for the east limb and EUVI-A for the west limb), and the Large-Angle and Spectrometric Coronagraph Experiment (LASCO; Brueckner *et al.* 1995) onboard SOHO to identify the associated mass ejections. As the active region transited the far side of the Sun, we also used the STEREO/SECCHI EUVIs to monitor its behavior, while the STEREO/SECCHI COR2 coronagraphs were used to detect the associated eruptions.

After careful inspection of these observations, we compiled 129 ejective events as being associated to the active region of interest. Among these, we included all kinds of white-light ejecta that were discernible from the background corona in running-difference images, and at least in two consecutive images. The angular width (AW) of each CME was measured in the set of coronagraphic images where the CME propagation was closer to the corresponding plane of the sky. For completeness, we also consulted the SOHO/LASCO CME Catalog (http://cdaw.gsfc.nasa.gov/CME_list) (Yashiro *et al.* 2004) and the Computer-Aided CME Tracking catalog (<http://sidc.oma.be/cactus/>) (CACTus; Robbrecht & Berghmans 2004).

All identified CME events are plotted in Figure 1a, with their AWs shown as a function of time. We choose to examine the CME AW because it is an attribute that is directly associated with the energy involved in the event, given that generally wider CMEs are more massive and faster (e.g. Gopalswamy 2010). The plot shows that there are periods of time that stand out from the rest, during which several wide CMEs are ejected in a few days. These bursts of CMEs are particularly noticed by the end of August, by mid-October, and during 10–14 November 2010.

4. Magnetic flux and current helicity

For those time intervals when the active region transited the front side of the Sun as seen from Earth, it was possible to investigate photospheric properties of the magnetic field. Magnetic flux evolution is expected to show correspondence with eruptive activity, given that flux emergence has been pointed out as a possible trigger of CME eruptions (e.g., van Driel-Gesztelyi & Green 2015). To examine such association, we plot in Figure 1b the positive, negative, and average total magnetic flux in the region as a function of time. The magnetic flux is computed using full-disk level 1.8 Michelson Doppler Imager (MDI; Scherrer *et al.* 1995) magnetograms. These data are the average of 5 magnetograms with a cadence of 30 seconds and a noise error of 20 G per pixel. They are constructed once every 96 minutes, being the error in the flux densities per pixel in the averaged magnetograms of 9 G. To find the AR flux, a polygonal contour defined by eye is fitted around the AR. The boundary of the contour is the sharp flux density change between the AR and the network field. Within this region the flux is calculated for all positive (negative) values above (below) 50 G (-50 G) giving the positive (negative) flux curve. The average flux curve is the summation of the positive and the absolute value of the negative curves divided by two. Because of projection effects involved in the magnetic flux determination, we only show values corresponding to the dates when the active region was on central meridian ± 4 days.

The first period of high ejective activity takes place while the region was on the far side of the Sun, when magnetograms are not available. However, as can be inferred from Figure 1b, the magnetic flux must have increased during the far-side passage from values of $\approx 1 \times 10^{22}$ Mx to more than 2.5×10^{22} Mx. Likewise, there is a rapid increase of magnetic flux in the fourth rotation, which matches the ejective activity in mid-October 2010. It must be noted that some of the local rapid changes in flux may be masked by other emergence/cancellation of flux in the region, since the flux that we plot has been integrated over the full area of interest. This is the case for the rapid emergence of active region NOAA 11123, which builds up a complex together with region 11121, and produces many CMEs during 10–14 November 2010.

Inspired by the work of Liu *et al.* (2016), we investigated the behavior of the current helicity H_c in connection with the eruptive activity. Temporal series of total unsigned H_c and mean H_c were obtained from the Space-weather HMI Active Region Patches (SHARPS; Bobra *et al.* 2014) data products, available at <http://jsoc.stanford.edu>. The H_c data series for the dates corresponding to the active region numbers shown in Table 1 have been plotted in Figures 1c and d. The total unsigned H_c in Figure 1c shows dips before or about the dates of the three periods with high eruptive activity, which is suggestive of a possible association between both phenomena. The mean H_c shows a similar behavior, except for the last rotation, which shows a peak rather than a dip. Violent changes of the mean H_c are however associated with all time periods of high eruptive activity.

5. Final remarks

The quadrature views provided by the STEREO spacecraft, combined with Earth's perspective from SDO and SOHO, offer the unique opportunity to track an active region and its ensuing CMEs while it traverses the far side of the Sun. For the first time, we have uninterruptedly tracked a long-duration active region for five solar rotations and identified its productivity in terms of white-light ejecta. The evolution of magnetic flux and current helicity in the region are inspected when possible, i.e. during

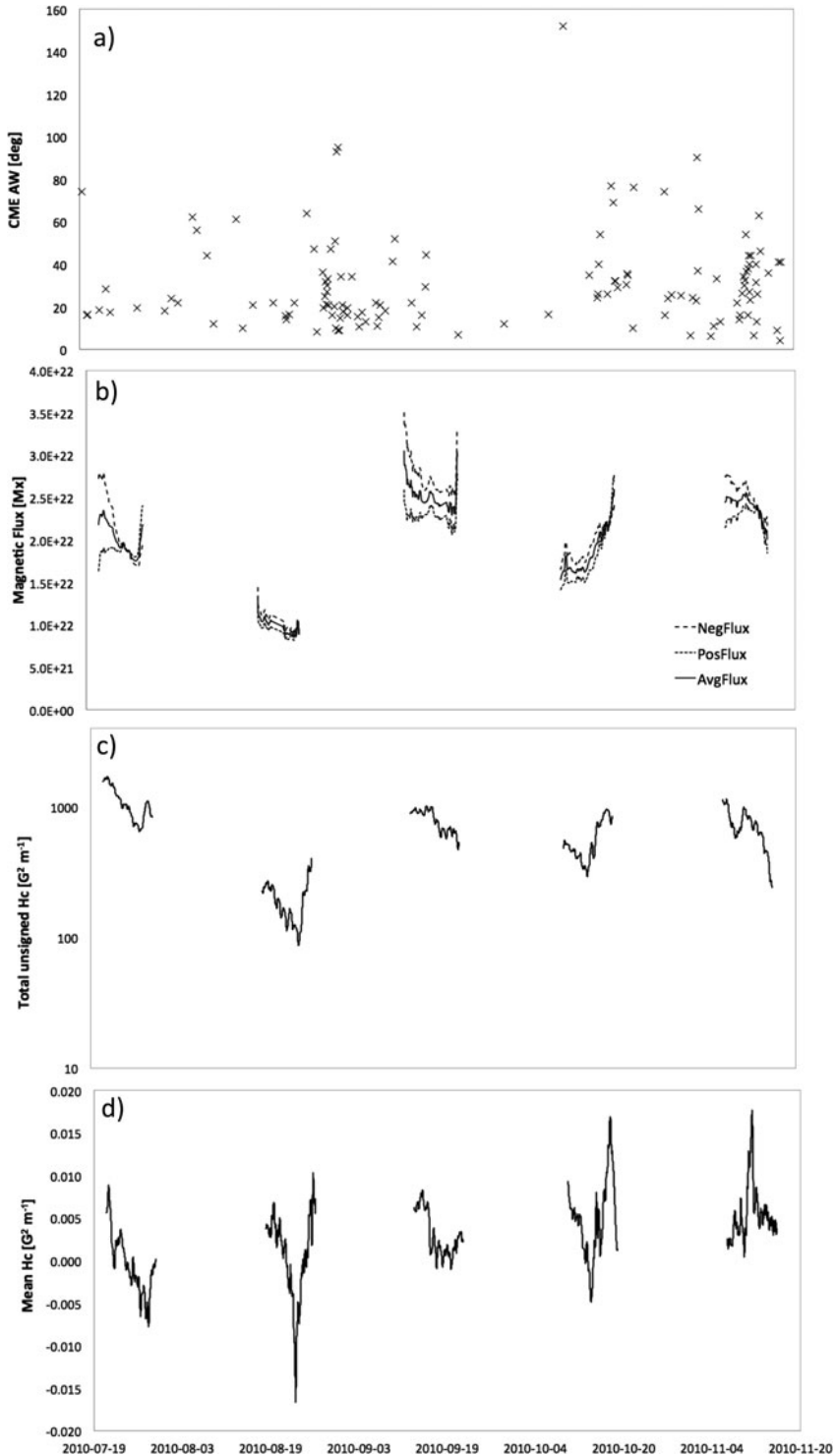


Figure 1. Temporal behavior of the eruptive activity and magnetic parameters associated with the active region during the investigated time interval. a) CME AW. b) Average magnetic flux (solid line), positive magnetic flux (dotted line), and negative magnetic flux (dashed line). c) Total unsigned current helicity H_c , in a logarithmic scale. d) Mean current helicity.

front-side transits of the region. The first results of this work in progress are suggestive of a correspondence between these data series and the gross amount of white-light ejecta, and are thus promising towards finding early indicators of CME production.

Acknowledgements

HC, CHM, MLF, and IC are members of the Carrera del Investigador Científico (CONICET). FML and MP are fellows of CONICET. The authors appreciate financial support from the Argentine grants PICT 2012-973 (ANPCyT) and PIP 2012-01-403 (CONICET). HC, LM, and FML thank support from project UTN UTI4035TC. The authors acknowledge the use of data from the STEREO (NASA), SDO (NASA), and SOHO (ESA/NASA) missions. These data are produced by the AIA, HMI, SECCHI, LASCO, and MDI international consortia.

References

- Bobra, M. G., Sun, X., Hoeksema, J. T., Turmon, M., Liu, Y., Hayashi, K., Barnes, G., & Leka, K. D. 2014, *Solar Phys.*, 289, 3549
- Brueckner, G. E. *et al.* 1995, *Solar Phys.*, 162, 357
- Cremades, H., Mandrini, C. H., Schmieder, B., & Crescitelli, A. M. 2015, *Solar Phys.*, 290, 1671
- Démoulin, P., Mandrini, C. H., van Driel-Gesztelyi, L., Thompson, B. J., Plunkett, S., Kovári, Z., Aulanier, G., & Young, A. 2002, *A&A*, 382, 650
- Domingo, V., Fleck, B., & Poland, A. I. 1995, *Solar Phys.*, 162, 1
- Forbes, T. G. 2000, *J. Geophys. Res.*, 105, 23153
- Gopalswamy, N. 2010, in: I. Dorotovic (ed.), *20th National Solar Physics Meeting*, p. 108
- Green, L. M., López fuentes, M. C., Mandrini, C. H., Démoulin, P., Van Driel-Gesztelyi, L., & Culhane, J. L. 2002, *Solar Phys.*, 208, 43
- Gopalswamy, N., Lara, A., Yashiro, S., Nunes, S., & Howard, R. 2003, in: A. Wilson (ed.), *Solar Variability as an Input to the Earth's Environment*, ESA Special Publication, 535, p. 403
- Guo, Y., Démoulin, P., Schmieder, B., Ding, M. D., Vargas Domínguez, S., & Liu, Y. 2013, *A&A*, 555, A19
- Howard, R. A. *et al.* 2008, *Space Sci. Revs.*, 136, 67
- Kaiser, M. L., Kucera, T. A., Davila, J. M., St. Cyr, O. C., Guhathakurta, M., & Christian, E. 2008, *Space Sci. Revs.*, 136, 5
- Lara, A., Gopalswamy, N., Xie, H., Mendoza-Torres, E., Pérez-EriQuez, R., & Michalek, G. 2006, *J. Geophys. Res.*, 111, A06107
- Lemen, J. R. *et al.* 2012, *Solar Phys.*, 275, L17
- Liu, L., Wang, Y., Wang, J., Shen, C., Ye, P., Liu, R., Chen, J., Zhang, Q., & Wang, S. 2016, *ApJ*, 826, 119
- Mandrini, C. H., Schmieder, B., Démoulin, P., Guo, Y., & Cristiani, G. D. 2014, *Solar Phys.*, 289, L2041
- Pesnell, W., Thompson, B. J., & Chamberlin, P. C. 2012, *Solar Phys.*, 275, 3
- Petrie, G. J. 2013, *ApJ*, 768, 162
- Riley, P., Schatzman, C., Cane, H. V., Richardson, I. G., & Gopalswamy, N. 2006, *ApJ*, 647, 648
- &Robbrecht, E. and Berghmans, D. 2004, *A&A*, 425, 1097
- Schrijver, C. J. & Zwann, C. 2000, *Irish Astronomical Journal*, 27, 234
- Scherrer, P. H. *et al.* 1995, *Solar Phys.*, 162, 129
- Scherrer, P. H. *et al.* 2012, *Solar Phys.*, 275, 207

- van Driel-Gesztelyi, L. & Green, L. M. 2015, *Living Rev. Sol. Phys.*, 12, 1
- Yashiro, S., Gopalswamy, N., Michalek, G., St. Cyr, O. C., Plunkett, S. P., Rich, N. B., & Howard, R. A. 2004, *J. Geophys. Res.*, 109, A07105
- Zuccarello, F., Guglielmino, S. L., & Romano, P. 2014, *ApJ*, 787, 57